SUPPLEMENTARY MATERIAL

Proton Dynamics in a Spark-Plasma Sintered $BaZr_{0.7}Ce_{0.2}Y_{0.1}O_{3-\delta}$ Proton Conductor investigated by Quasi-elastic neutron scattering

Received 00th January 20xx,
Accepted 00th January 20xx

DOI: 10.1039/x0xx00000x

Supplementary Material

J. Wallis[a*], A. Kruth[a], F. Demmel[b]

1 Characteristics of the $BaZr_{0.7}Ce_{0.2}Y_{0.1}O_{3-\delta}$ sample

The $BaZr_{0.7}Ce_{0.2}Y_{0.1}O_{3-\delta}$ (BZCY72) sample investigated by QENS in the main article exhibited a high relative density of 97.9 % as determined geometrically from the sample dimensions where a theoretical density of 6.20 g/cm³ was used.
Further characterization of the microstructure was carried out by means of an JSM 7500 Field emission SEM. Fig. 1 presents the grain structure of BZCY72 prepared by Spark Plasma Sintering (SPS). The average grain size determined by multiple SEM images is 222 ± 98 nm. The grains are irregular in size and shape indicating abnormal grain growth during the SPS process. The remaining porosity is composed of intergranular pores and spacing between adjacent pores. The grain boundaries appeared to be free of impurities, although the resolution was not sufficient to establish this with high certainly.
XRD measurements confirm a high phase purity of the rhombohedral BZCY72 main phase, fig. 2. The space group is $R\bar{3}c$ with lattice parameters of a = 6.014 and c = 14.704. A minor impurity is carbon (PDF 00-001-0640) due to the preparation method containing the sample inside a carbon die. Another impurity at 2θ = 28.9° matches Y_2O_3 (PDF 00-041-1105). The crystallite size was on average 76 ± 8 nm and the calculated B – O bond length from Rietveld refinement was 2.13 Å.

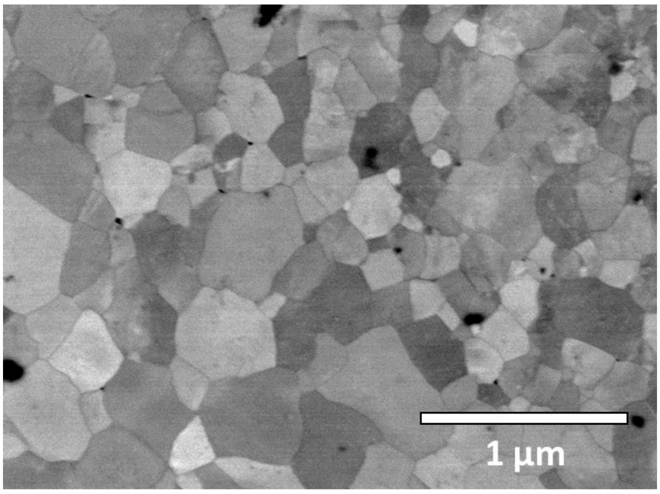

Fig. 1 SEM Image of the polished cross section of the BZCY72 sample prepared by SPS.

2 TGA measurements

TGA Measurements were carried out by a STA instrument (STA7200RV, Hitachi) for 170-200 mg of powder using a Pt pan. The samples were heated at 5 °C/min from 40 °C to 950 °C under a dry Ar atmosphere with a gas flow of 100 ml/min, while the weight change was recorded simultaneously. After reaching 950 °C the temperature was held for 6 h and then subsequently cooled at 5 °C/min to 40 °C, which was held again for 20 min.
Afterwards the argon was saturated with water vapor (pH_2O = 19.95 kPa) and the increased weight was recorded. The weight change is directly related to the water uptake and therefore the protonic defect concentration. Weight traces and protonic defect concentration are related as follows:

$$[OH^{\bullet}] = \frac{2\ \Delta m\ M_{oxide}}{m_{oxide}\ \ M_{H_2O}} \qquad (1)$$

[a] Leibniz Institute for Plasma Science and Technology, Felix-Hausdorff-Str. 2, 17489 Greifswald, Germany
[b] ISIS Facility, Rutherford Appleton Laboratory, Didcot, OX11 0QX, United Kingdom
*Corresponding author

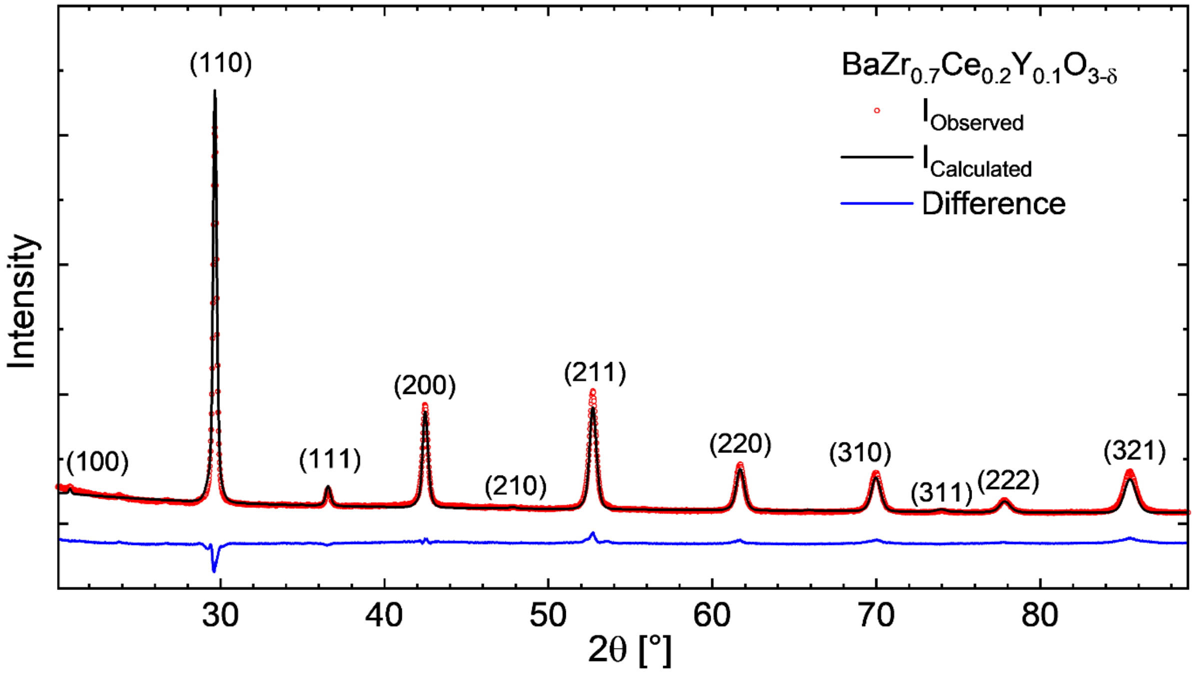

Fig. 2 XRD pattern of the BZCY72 sample prepared by SPS represented as red dots. The solid black line is the calculated intensity by a Rietveld refinement with the difference between the two intensities as blue solid line. All peaks are labeled with their corresponding miller indices.

where M_{oxide} and M_{H2O} are molecular weights of the oxides and water, Δm and m_{oxide} are weight change and weight of the specimen, respectively.

For the BZCY72 sample, a weight gain of 0.59 % was recorded between 230 °C and 420 °C, corresponding to a defect concentration $[OH^{\bullet}] \approx 0.187$ within this temperature regime, which is in good accordance with the value of 0.2 obtained from Neutron Compton spectroscopy (1).

3 Impedance spectroscopy

The impedance data was fitted with the using an equivalent circuit that consists of a resistor *R* and a constant phase element or CPE connected in parallel: (R_1Q_1) (R_2Q_2) (R_3Q_3), where each parallel circuit represents a specific phenomenon of the inspected system beginning with the bulk at high frequencies in with the resistance R_1, followed by the grain boundary contribution at intermediate frequencies and the electrode at low frequencies, according to the Boukamp circuit description code (2). The complex impedance of a CPE element and the quasi-equivalent capacity of a RQ element are given by equation 2 and 3, respectively:

$$Z(j,\omega) = \frac{1}{(j\omega)^n Q_0} \quad (2)$$

$$C = R^{\left(\frac{1}{n}-1\right)} Q^{\left(\frac{1}{n}\right)} \quad (3)$$

where $0 \leq n \leq 1$. The CPE represents a capacitor when n = 1 and a resistor for n = 0. ω is the angular frequency and j

The resistivity ρ and conductivity σ of the sample and its compartments can be calculated by:

$$\sigma = \frac{1}{\rho} = \frac{L}{RA} \quad (4)$$

taking the samples thickness L and electrode area A into account. This is also known as the geometric factor, correcting the data for sample dimensions. For further interpretation the imaginary (capacitive) impedance $-Z''$ is plotted as a function of the real (resistive) part of the impedance Z' as a Nyquist plot. Another IS data representation is the Bode plot where Z is plotted vs the frequency *f*. In addition, within complex systems it is often meaningful to calculate the electric modulus $M^* = M' + jM''$ to give emphasis to elements with small capacitances:

$$M^* = j\omega C_0 Z^* \quad (5)$$

where C_0 is the vacuum capacitance.

Fig. 3 presents the Nyquist plot of the BZCY72 sample investigated in the main article at 300 °C. The sample can be separated into two components as indicated by the equivalent circle fits. The extracted capacities are C_1 = 8.2 pF and C_2 = 354 pF for the bulk and grain boundary, respectively.

Please do not adjust margins

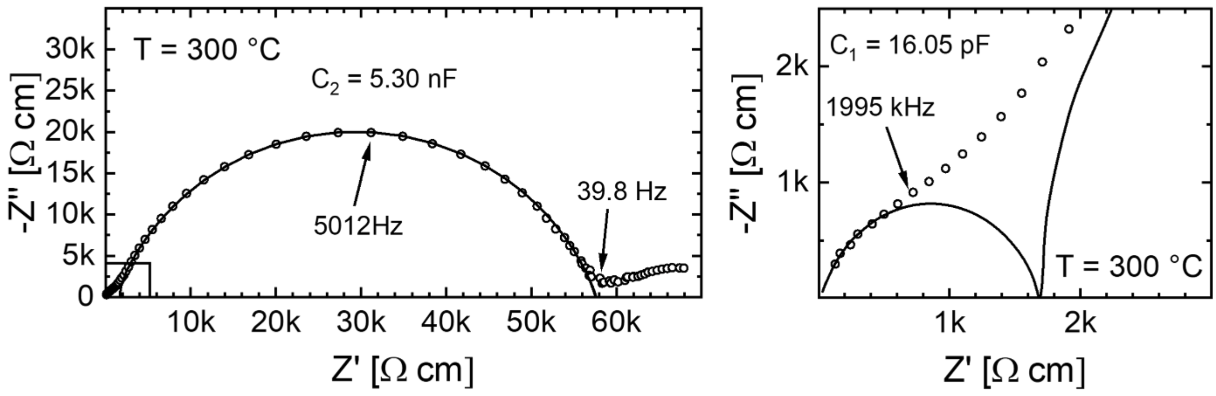

Fig. 3 Complex plane plot (Nyquist plot) of the BZCY72 pellet prepared by SPS at T = 300 °C. The capacities are given within the figure. On the right side the high-frequency region is shown to emphasize the bulk contribution. The solid black line represents a fit using individual resistances and constant phase elements in parallel.

4 References

1. Wallis J, Kruth A, Da Silva I, Krzystyniak M. Nuclear dynamics in BaZr0. 7Ce0. 2Y0. 1O3− δ proton conductor as observed by neutron diffraction and Compton scattering. Journal of Physics Communications. 2020;4(4):045004.
2. Boukamp BA. Electrochemical impedance spectroscopy in solid state ionics: recent advances. Solid state ionics. 2004;169(1-4):65-73.